11th International Symposium on Magnetic Bearings
August 26-29, Nara, Japan

NUMERICAL INVESTIGATION OF AMB SUPPORTED ROTOR INTERACTION WITH AUXILIARY BEARINGS

Lei Xie , Rainer Nordmann
Mechatronik im Maschinenbau, Technische Universität Darmstadt,
Petersenstr. 30, 64287 Darmstadt,Germany
nordmann@mim.tu-darmstadt.de, xie@mim.tu-darmstadt.de
Beat Aeschlimann
Mecos Traxler AG,Industriestrasse 26,CH-8404 Winterthur, Switzerland
Beat.Aeschlimann@mecos.com

ABSTRACT
This paper describes numerical analysis of interaction between rotor and auxiliary bearing due to high transient overloads. When the fast spinning rotor interacts with the auxiliary bearing that does not move, some critical states of motion are possible. One of these motions, backward whirl, reaches very high frequencies and thus can produce very high loads on rotor and bearings, which can lead to the destruction of the machine.

The detailed model of the AMB supported rotor auxiliary bearing system considers discontinuous stiffness caused by bearing clearance effects, auxiliary bearing fixed or flexible mount types, nonlinear Hertzian contact stiffness and Coulomb friction forces. Numerical investigations as time history, orbit diagram, bifurcation diagram, Poincaré section diagram are proposed to study the system parameters which extremely influence the whole dynamic response. One of the important parameters, rotor driving frequency, can be modelled as time variable parameter in the detailed system model. Moreover, parameters used in the detailed model discussed in this paper obtained from experimental test rig.

INTRODUCTION
Auxiliary bearings play an indispensable role in active magnetic bearings (AMBs) supported rotor systems. They support high speed spinning rotor in the case of AMBs fail to work, or transient load conditions [1]. When the high speed spinning rotor interacts with the stationary auxiliary bearings, a fatal critical state of motion, backward whirl is possible. During backward whirl, rotor reaches very high frequencies and thus can produce very high loads on rotor and bearings, which can lead to the destruction of the machine [2]. So, it is important to study detailed model of the interaction between rotor and auxiliary bearing in order to explore which factors are essential to this kind destructive failure and find an appropriate design to prevent it.

In recent years many studies have been carried out about the nonlinear model of interaction between rotor and auxiliary bearings. The work of F. F. Ehrich in publication [3] has clearly demonstrated nonlinear model due to bearing clearance. Full annular rubbing interaction between rotor and seal, including synchronous or reverse (backward) precessions, has been analytical discussed by D. E. Bently, J.J. Yu in publication [4]. Kirk gave a very detail review of the analysis method of transient rotor drop down to auxiliary bearing for AMBs rotor system [5]. M. Orth developed a modelling tool called ANEAS to simulate AMBs rotor system and study the effect of the initial start point of rotor and behaviour of rotor after drop down [1,6]. P. S. Keogh, M. O. T. Cole developed experimental procedures to study the contact dynamic response with consideration of misalignment [7]. Chaotic and regular vibration of the rotor due to bearing clearance has been extensively investigated in publication [8] by Karpenko.

In this paper, the detailed model of the AMBs supported rotor auxiliary bearing system considers discontinuous stiffness caused by bearing clearance effects, nonlinear Hertzian contact and Coulomb friction forces; rotor driving frequency can be a time varying parameter; The auxiliary bearings could be fixed and compliant mounted in machine housing. Numerical investigations as time history, orbit diagram, bifurcation diagram, Poincaré section diagram are proposed to study the system parameters which extremely influence the whole dynamic response. A numerical investigation of AMBs supported rotor interaction with auxiliary bearing system is implemented in commercial software MATLAB.

TEST RIG

The test rig consists of a rotor, which is radically suspended with two AMBs. Two pairs of inductive sensors are mounted to the test rig to measure the radial displacement of the rotor, which have to be known for controlling the AMBs. Two single row deep groove ball bearings made by SKF (SKF 6004) are assembled to the test rig as auxiliary bearing. The air gap between the rotor and the bearing is 0.3 mm. A motor provide the drive power to rotor. The maximal driving frequency reaches 500 Hz (30000 rpm). The first bending eigenfrequency for the free-free rotor is approximately 1600 Hz; the first bending eigenfrequency for the fixed-fixed rotor is approximately 696 Hz. Further information about test rig is introduced in [9]. Table 1 lists the most important parameters of the test rig, which has been also used in the numerical investigation in this paper.

TABLE 1: Parameters of the test rig

Rotor	
Mass of the rotor	3.36 kg
Polar moment of inertia	0.001 kgm^2
Transverse moment of inertia	0.017 kgm^2
Unbalance eccentricity	0.0292 mm
Clearance	0.3 mm
AMB	
Radial static stiffness	2.4670e+6 N/m
Radial static damping coefficient	100 Ns/m
Auxiliary bearing	
Mass of the auxiliary bearing	0.069 kg
Coefficient of Coulomb friction	0.015
Local stiffness of Hertzian contact	2.4e+9N/m$^{3/2}$
Damping coefficient of Hertzian	5

SYSTEM MODEL

In this paper, we introduce a rigid rotor to analyze the rotor dynamic and the influence of the system parameters. The unbalance of the rotor provides the harmonic excitation with varying driving frequency. Rotor could be considered as a rigid rotor and neglected the gyroscopic effect. The static stiffness of active magnetic bearing is depended on controller parameters the rotor position and the coil currents. Under some special conditions such as active magnetic bearing failure or high transient overloads etc., rotor interacts with auxiliary bearing, and then additional contact force and friction force are generated between rotor and auxiliary bearing.

A mathematical model of the AMB supported Rotor-Auxiliary bearing system is shown in Fig. 1. The absolute coordinate system is OXY; the displacement of the centre rotor Or in horizontal direction and vertical direction are denoted as x and y; the centre of the auxiliary bearing Ob is at position [xb , yb], which are not equal to zero when the auxiliary bearing is misalignment with absolute coordinate system. The clearance between rotor and auxiliary bearing is Cs. AMBs provide spring force and damping force, whose stiffness and damping are respectively $k1$ and $d1$. $k2$ and $d2$ are supporting stiffness and damping of the auxiliary bearing respectively which are provide by machine housing or support component. $\tilde{k}c$ and $\tilde{d}c$ are respectively contact stiffness and damping which could be liner contact stiffness or nonlinear Hertzian contact stiffness.

When the auxiliary bearings are mounted directly with the machine housing, it could be assumed as fixed mounted auxiliary bearings; so the supporting stiffness is much higher than the contact stiffness, therefore, the supporting stiffness and damping could be ignored. Otherwise, when the auxiliary bearings are compliantly mounted on the machine housing, the supporting stiffness and damping must be taken into account in the system mathematical model.

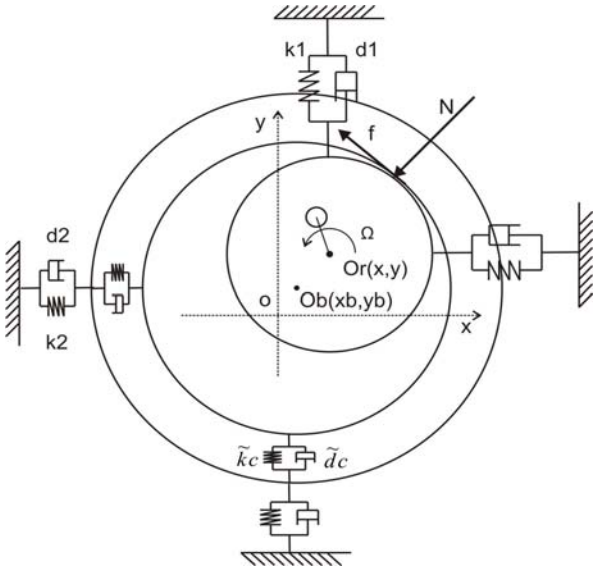

FIGURE 1: Model of the system

The second order equations of motion for this type rotor model can be described in two states due to clearance between rotor and auxiliary bearing, one is without interaction (State 1) between rotor and auxiliary

bearings, and the other (State 2) is with the interaction between rotor and auxiliary bearings.

Equations of motion of AMBs supported rotor with fixed mounted auxiliary bearing

State 1:

$$m\ddot{x}(t)+d1\dot{x}(t)+k1x(t)=F\cos(\Omega t)$$
$$m\ddot{y}(t)+d1\dot{y}(t)+k1y(t)=F\sin(\Omega t)$$

State 2:

$$m\ddot{x}(t)+d1\dot{x}(t)+k1x(t)=F\cos(\Omega t)+N_x+f_x$$
$$m\ddot{y}(t)+d1\dot{y}(t)+k1y(t)=F\sin(\Omega t)+N_y+f_y$$

Equations of motion of AMBs supported rotor with compliant mounted auxiliary bearing

State 1:

$$m\ddot{x}(t)+d1\dot{x}(t)+k1x(t)=F\cos(\Omega t)$$
$$m\ddot{y}(t)+d1\dot{y}(t)+k1y(t)=F\sin(\Omega t)$$
$$m_b\ddot{x}(t)+d2\dot{x}(t)+k2x(t)=0$$
$$m_b\ddot{y}(t)+d2\dot{y}(t)+k2y(t)=0$$

State 2:

$$m\ddot{x}(t)+d1\dot{x}(t)+k1x(t)=F\cos(\Omega t)+N_x+f_x$$
$$m\ddot{y}(t)+d1\dot{y}(t)+k1y(t)=F\sin(\Omega t)+N_y+f_y$$
$$m_b\ddot{x}(t)+d2\dot{x}(t)+k2x(t)=-N_x-f_x$$
$$m_b\ddot{y}(t)+d2\dot{y}(t)+k2y(t)=-N_y-f_y$$

where, m is mass of the rotor. mb is mass of the auxiliary bearing. Ω is rotor driving frequency. In many studies, the rotor driving frequency Ω is assumed as a constant value, but in actual condition, it can not be simplified as a constant, it is a variable depend on many factors. In [10], authors introduced experimental formulas for the deceleration of the driving speed due to the aerodynamic torque in the case of power failure. In this paper, the rotor driving frequency could be modeled as a time variable parameter. me is unbalance of the rotor. Unbalance force can be modeled as $F=\Omega^2 me$; N_x, N_y are normal contact force components in horizontal and vertical directions respectively; f_x, f_y are tangential friction force components in horizontal and vertical directions respectively.

For a simplified model, the contact force N between rotor and auxiliary bearing can be considered as ideal elastic force, which is linear with the non-negative radial penetration

$$\delta=\sqrt{(x-xs)^2+(y-ys)^2}-Cs,$$

with contact stiffness $\tilde{k}c$, so contact force is as follows:

$$N=\tilde{k}c\cdot\delta$$

Friction force f between two contact surfaces is followed Coulomb law $f=\mu N$, here μ is the friction coefficient between rotor and auxiliary bearing.

It is worth to mention that when contact is between two perfectly flat surfaces, the area of contact zone does not change during the time of impact, so the ideal linear elastic contact law probably applies. The contact type between rotor and auxiliary bearing is cylinders in longitudinal contact. In order to get more actual physical contact model, we also studied Hertzian nonlinear contact in the detailed AMB-rotor-auxiliary bearing model. In [11], the authors introduced the Hertzian nonlinear contact model.

During rotor contacts with auxiliary bearing, the normal contact force between rotor and auxiliary bearing can be written as

$$N=k\delta^{3/2}+\frac{3}{2}\alpha k\delta^{3/2}\dot{\delta}=\tilde{k}c(\delta,\dot{\delta})+\tilde{d}c(\delta,\dot{\delta}).$$

Here δ is radial penetration, $\dot{\delta}$ is penetration δ derivative with respect of time, k is local stiffness parameter, α is damping parameter. With the result of experiment measured contact force, detail estimation method of the contact force by using Hertzian nonlinear contact theory is introduced in order to get parameters k local stiffness and α damping coefficient in [9]. The author also assumed that the contact could be two sphere contacts for practical purpose, exponent of δ is to equal to 3/2, which is dependent on the type of the contact.

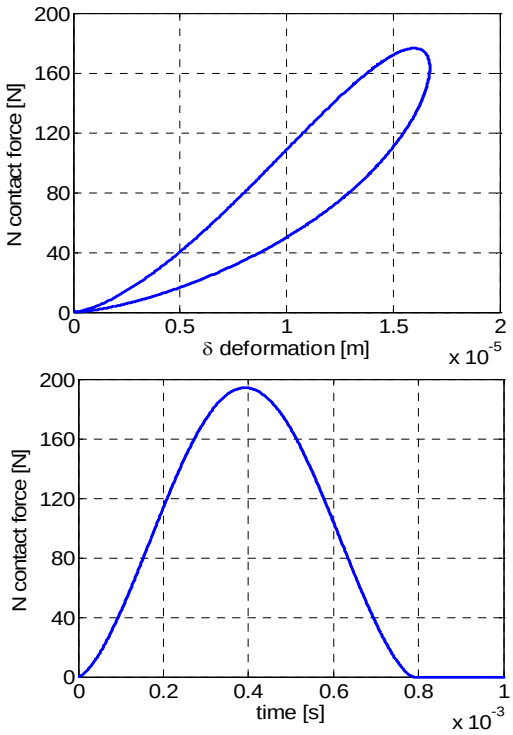

FIGURE 2: Hertzian nonlinear contact

Figure 2 shows simulation results of an example of Hertzian nonlinear contact, local stiffness parameter

k is about 2.4×10^{9} N/m$^{3/2}$ and damping parameter α may be determined for small impact velocities from the linearized relation between coefficient of restitution and impact velocity [11]. Fig. 2 (top) shows the hysteretic relation between normal contact force N and penetration δ. The nonlinear contact stiffness varies from 2.86×10^{5} N/m to 1.16×10^{7} N/m during the contact under some special initial conditions. From Fig.2(bottom), the nonlinear contact force is continually changing with time, which is different with linear contact.

SIMULATION RESULTS ANALYSIS

The detailed model of the AMB supported Rotor-Auxiliary bearing system has considered important system parameters such as unbalance of rotor, driving frequency which could be time variable and invariable, supporting stiffness and damping of auxiliary bearing, stiffness and damping of contact, clearance, misalignment between rotor and auxiliary bearing etc. Since the driving frequency is one of the most convenient parameters to be controlled in the build up test rig, it has been chosen as a parameter of study in this work. Some important parameters of the detailed model are obtained from test rig which is introduced in section 1 and listed in Table 1.

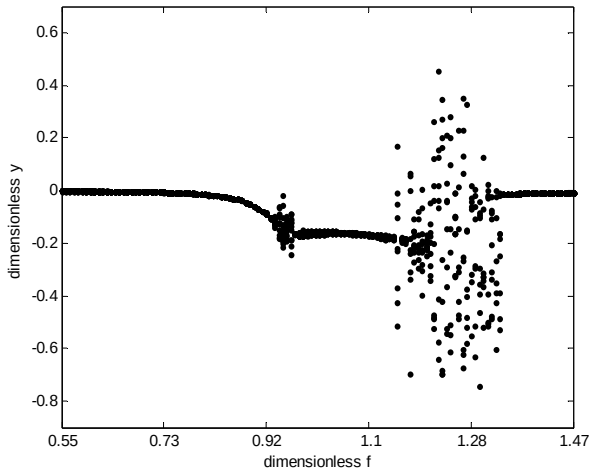

FIGURE 3: Bifurcation diagram

The above derived equations of motion were first mathematically transferred into a set of first-order differential equations [12]. The well-known Runge-Kutta method is used to solve these equations. Plenty cycles were allowed before data was analysed, to ensure that a steady state solution had been achieved. Moreover, for numerical solution, the initial conditions are very important for successive and economic computational solution. Particularly for nonlinear systems, different initial conditions mean totally different solutions. The control parameter was increased in small steps, each step starting with same initial conditions

The equations of motion derived in above section are nondimensionalized in order to compare and discuss numerical simulation results with different control parameters conveniently. The time is nondimensionalized by using natural frequency of the rotor system; the displacements, such as horizontal and vertical displacements of rotor centre, are nondimensionalized by employing the clearance between rotor and auxiliary bearing.

A bifurcation diagram is a very effective method to reflect the motion change by control parameter change. In order to compute a bifurcation diagram, a control parameter dimensionless driving frequency is varied from 0.55 to 1.5 at a constant step size 0.0073. As Fig.3 shows, the numerical simulation results obtained from the study system model represent complex behaviours with different dimensionless driving frequencies. In the low dimensionless driving frequency range from 0.55 to 0.91, period one motion is observed. At around 0.92 it flips to period three motion, then after a slender range period one motion, it shows a possible band of chaotic motion between 0.94 and 0.96. Period two motion is observed in the region [0.97 1.17]. With increase of the control parameter, the motion of the system model becomes more complicated. From 1.17 to 1.33, chaotic motion was predominant, but period two motion, period four motion are observed at some specific values of the control parameter as well. If the dimensionless driving frequency is beyond 1.34, the bifurcation diagram shows a transition from chaotic motion into period one motion obviously.

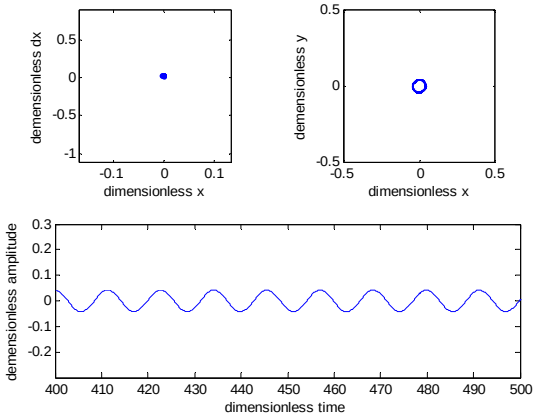

FIGURE 4: Poincaré section diagram, rotor orbit, rotor time history in dimensionless coordinates at dimensionless driving frequency 0.55 (piecewise linear contact model)

The simulation results of the system mathematical model show the period one, period two, period four and chaotic motion, etc. Figures 4 - 7 show the Poincaré section diagrams, the rotor orbits, the rotor time histories in dimensionless coordinate at different driving frequency of 0.55, and 1.28 respectively. When the dimensionless driving frequency is at 0.55, the motion is regular and periodic one as shown the orbit map in Fig.4(right) and time history in Fig.4(down). And there are many points clustered into one point in the Poincaré section diagram in Fig.4(left). The system response is presented a period one motion. Contact force of the system is modelled as pricewise ideal elastic linear contact when rotor interacts with fixed mounted auxiliary bearing.

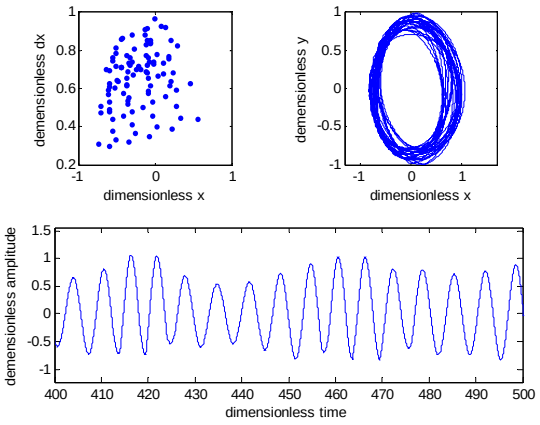

FIGURE 5: Poincaré section diagram, rotor orbit, rotor time history in dimensionless coordinates at dimensionless driving frequency 0.55 (Hertzian nonlinear contact model)

As shown in Fig.5, the dimensionless driving frequency is also at about 0.55. But, the simulation results show obvious difference with the Fig.4. From Poincaré section diagrams Fig.5(left) and the time history of the dimensionless rotor displacement Fig.5(down), motion of the study model is chaotic. The results shown in Fig.5 are of the revised model whose contact force is modelled as nonlinear Hertzian contact. Except the contact force model, the other parameters of these two models are same.

Figure 6 and Fig. 7 show simulation results at 1.28 dimensionless driving frequencies of the piecewise linear contact system model and hertzian nonlinear contact system model respectively. Fig.6 and Fig.7 both show chaotic motion. The rotor orbit and time history is obviously chaotic, Poincaré section diagram shows a geometrically fractal like structure. Based on Figs 3-7 one can say that the detailed nonlinear AMB-rotor-auxiliary bearing system represents the complex dynamic characters at different driving frequencies obviously. But it is worthy to mention that the other parameters of the model and model type are also very important parameters, which may be related to the stability of rotor motion directly.

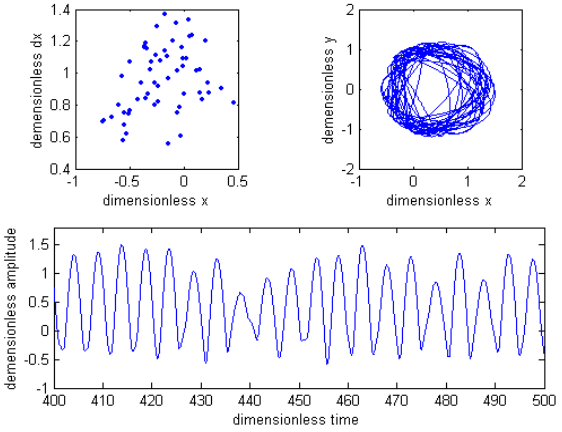

FIGURE 6: Poincaré section diagram, rotor orbit, rotor time history in dimensionless coordinates at dimensionless driving frequency 1.28 (piecewise linear contact model)

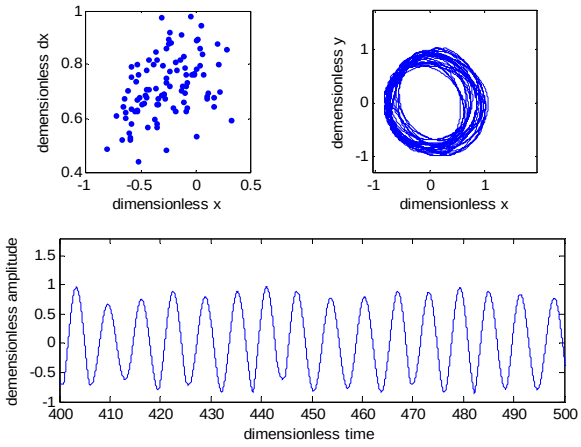

FIGURE 7: Poincaré section diagram, rotor orbit, rotor time history in dimensionless coordinates at dimensionless driving frequency 1.28 (Hertzian nonlinear contact model)

Figure 8 presented the simulated dimensionless contact force of the piecewise linear contact model and nonlinear hertzian contact model respectively. Fig 8 (top) is dimensionless piecewise linear contact force which was calculated with the dimensionless rotor driving frequency at 1.28. From Fig.8 (top) it can be seen that rotor dose not continuously contact with auxiliary bearing, when there is no interaction between rotor and auxiliary bearing, the non negative contact

force is equal to zero from dimesionless time 400 to 500. And the piecewise contact force at this situation is quasi period as Fig.8 (top) shown. Fig.8 (bottom) is dimensionless hertzian contact force which is simulated with dimensionless rotor driving frequency at 0.55. It can be clearly seen that the rotor continuously contacts with auxiliary bearing from dimensionless time 400 to 500, and it is quite chaotic. It may be that the hertzian contact force is more complicated than the piecewise linear contact which is only depend on the contact stiffness and the value of penetration; but the hertzian nonlinear contact is not only depend on some system parameters, local stiffness parameter and damping parameter, but also depend on the penetration and its derivative with respect to time.

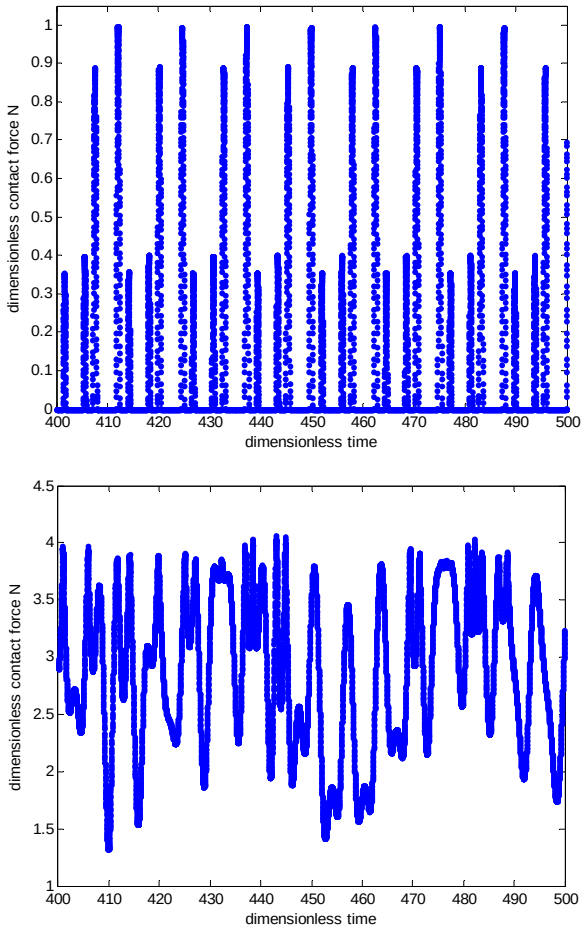

FIGURE 8: Simulated dimensionless contact force

CONCLUSION

Through numerical investigations presented in this paper, it is found that the rotor-AMB-auxiliary bearing system undergoes complicate motion behaviour. The detailed model which considers discontinuous stiffness caused by bearing clearance effects, nonlinear Hertzian contact stiffness Coulomb friction forces and time varying driving frequency, fixed and compliant mounted auxiliary bearing were developed in this paper. Bifurcation diagrams, Poincaré section diagram and were used to analyse these complex motions. Further researches will focus on the studies of other important system parameters and experimental verification on the build-up test rig.

REFERENCE

[1] M. Orth, R. Nordmann, ANEAS - A Modeling Tool for Nonlinear Analysis of Active Magnetic Bearing Systems Mechatronics 2002 Conference, Dec. 2002, Berkeley, California

[2] M. Helfert, M. Ernst, R. Nordmann, B. Aeschlimann, High-Speed Video Analysis of Rotor-Retainer Bearing Contacts Due to Failure of Active Magnetic Bearings, 10th International Symposium on Magnetic Bearings, 21. – 23. August 2006, Martigny, Switzerland

[3] F.F. Ehrich, Stator Whirl With rotors in bearing Clearance, ASME Journal of engineering for Industry, 1967,August:381–390.

[4] D. E. Bently, Paul Goldman, John J. Yu, Full Annular rub in mechanical seals Part II: Analytical Study, International Journal of Rotating Machinery, 8(5):329-336,2002

[5] R. G. Kirk, Evaluation of AMB Turbomachinery Auxiliary Bearings, ASME Journal of Vibration and Acoustics, 121(1999), 156-161

[6] M. Orth, R. Erb, R. Nordmann, Investigations of the Behavior of a Magnetically Suspended Rotor during Contact with its Retainer Bearings, Proceedings of 7.ISMB, S. 33 - 38, Zürich, Switzerland

[7] P.S. Keogh, M.O. T. Cole, Contact Dynamic Response with Misalignment in a Flexible Rotor/ Magnetic bearing System, Journal of Applied Mechanics,128(2006),362-369

[8] E. V. Karpenko, M. Wiercigroch, M. P. Cartmell, Regular and chaotic dynamics of a discontinuously nonlinear rotor system. Chaos, Solitons and Fractals, 13(2002), 1231-1242

[9] M. A. Fumagalli, Modelling and measurement analysis of the contact interaction between a high speed rotor and its stator, ETH Zürich, dissertation Nr.12509, 1997

[10]J. Schmied, J.C. Pradetto, Behaviour of a One Ton Rotor Being Dropped into Auxiliary Bearings, 3rd International Symposium on Magnetic Bearings, p.145-156, Alexandia,USA,

[11] K.H. Hunt, F.R. Crossley, Coefficient of restitution interpreted as damping in vibroimpact, ASME Journal of Applied Mechanics, 42 (1975),440-445

[12] R. Gasch, R. Nordmann, H. Pfützner: Rotordynamik. Springer Verlag,2002